

Adaptive Quickest Estimation Algorithm for Smart Grid Network Topology Error

Yi Huang, *Student Member, IEEE*, Mohammad Esmalifalak, *Student Member, IEEE*, Yu Cheng, Husheng Li, *Member, IEEE*, Kristy A. Campbell, and Zhu Han, *Senior Member, IEEE*

Abstract—Smart grid technologies have significantly enhanced robustness and efficiency of the traditional power grid networks by exploiting technical advances in sensing, measurement, and two-way communications between the suppliers and customers. The state estimation plays a major function in building such real-time models of power grid networks. For the smart grid state estimation, one of the essential objectives is to help detect and identify the topological error efficiently. In this paper, we propose the quickest estimation scheme to determine the network topology as quickly as possible with the given accuracy constraints from the dispersive environment. A Markov chain-based analytical model is also constructed to systematically analyze the proposed scheme for the online estimation. With the analytical model, we are able to configure the system parameters for the guaranteed performance in terms of the false-alarm rate (FAR) and missed detection ratio under a detection delay constraint. The accuracy of the analytical model and detection with performance guarantee are also discussed. The performance is evaluated through both analytical and numerical simulations with the MATPOWER 4.0 package. It is shown that the proposed scheme achieves the minimum average stopping time but retains the comparable estimation accuracy and FAR.

Index Terms—Bad data detection, network topology, signal detection, signal estimation, smart grid.

I. INTRODUCTION

THE DEVELOPMENT of the smart grid has grown rapidly in the recent years because of its promising economic, environmental, and social benefits [1]. With the aid of modern communication technologies, the future power grid has the capability of supporting two-way information and electricity flow, resolving the power outages efficiently, expediting renewable energy integration into the grid [2], and empowering people with better tools for optimizing their energy consumption.

Manuscript received March 26, 2012; accepted January 23, 2013. Date of publication July 3, 2013; date of current version May 22, 2014.

Y. Huang, M. Esmalifalak, and Z. Han are with the Department of Electrical and Computer Engineering, University of Houston, Houston, TX 77004-4005 USA (e-mail: yhuang23@uh.edu; hanzhu22@gmail.com).

Y. Cheng is with the Department of Electronics and Computer Engineering, Illinois Institute of Technology, Chicago, IL 60616-3793 USA.

H. Li is with the Department Electrical Engineering and Computer Science, University of Tennessee, Knoxville, TN 37996-2250 USA (e-mail: husheng@eecs.utk.edu).

K. A. Campbell is with the Department of Electrical and Computer Engineering, Boise State University, Boise, ID 83725 USA (e-mail: krisCampbell@boisestate.edu).

Color versions of one or more of the figures in this paper are available online at <http://ieeexplore.ieee.org>.

Digital Object Identifier 10.1109/JSYST.2013.2260678

The state estimation plays a major role in building such real-time models of power grid networks. Two types of measurement data are collected for state estimation in modern energy management systems (EMSs) of smart grid networks, namely: 1) the status data of switches and breakers and 2) the analog data of bus voltage, power injection, power flow, and reactance. The status data are used to determine the real-time topology of the network. The analog data are used to determine the loading/voltage profile of the line and transformer. However, both status and analog data are distortive because of the missing data, communication errors, or measurement errors. Errors in status data will show up as errors in the network topology, which will also cause the state estimation errors. In practice, the tree search algorithm [3], [4] to detect the erroneous data for the network topology processor is widely implemented. The authors in [5] applied the sequential search method through the network graph. In [6]–[8], the authors proposed the methods via using state estimation results for the topology error detection. Although the techniques are improved, the computational complexity of most existing approaches for the determination of topology error is high in practice.

The EMS needs to efficiently combat the topological error in a real-time manner to timely prevent further damage to the entire network [9]–[11]. In other words, the network topology should be determined as quickly as possible so that one can detect/identify the erroneous data to maintain a reliable database for the state estimator; otherwise, erroneous data can result in topology errors that invalidate the whole real-time modeling process on smart grid networks. This type of estimation problem can be solved via applying the quickest detection (QD) concept from [12]. The QD aims to determine a change of the observed statistics as quickly as possible based on online observations, the user-defined decision rules, and the requirement of detection accuracy. The decision rules need to be properly designed to optimize the tradeoff between the stopping time and decision accuracy. The authors in [13] utilized the adaptive nonparametric QD test to address the real-time malicious data attack on smart grid state estimation. The cognitive radio spectrum sensing with unknown parameters of primary user was described in [14]. In [15], the authors utilized the nonparametric cumulative sum (CUSUM) test with a Markov chain-based model to address the real-time backoff misbehavior problem and study the performance of the CUSUM detector in IEEE 802.11 networks. The authors in [16] combined the QD technique with the statistical hypothesis test for detecting abnormal change.

In this paper, we employ the *adaptive estimation algorithm* to help detect and identify the topological error efficiently for smart grid estimation. The proposed scheme is able to accomplish the following: 1) execute the demodulation of mutually interfering streams of information that is produced by all buses in the power network and, then, 2) determine the current network topology as quickly as possible without violating the given constraints such as a certain level of estimation accuracy that includes false alarm. With knowledge of the present network topology, one can explicitly determine and identify the topology error in an efficient way. Furthermore, we develop an analytical model for the proposed algorithm that provides theoretical guidance for quantitative performance analysis. With the analytical model, it provides us the insight on system parameter configuration for the online quickest estimation. System parameters can also be computed for guaranteed performance in terms of fundamental performance metrics: the false-alarm rate (FAR) and missed detection ratio (MDR) under a detection delay constraint. In other words, our analytical model can guide us to configure a detection system based on some detection performance requirement. The Markov chain-based analytical model for the proposed scheme involves two different transition probability matrices (TPMs): One is under the normal state environment, and the other one is under the malicious data attack. The normal TPM can help in determining the initial state as well as FAR. With the initial states, the MDR can be analyzed by using the TPM under attack. The performance of the proposed algorithm is evaluated by both mathematic analysis and numerical simulation. It is demonstrated in terms of fundamental metrics (e.g., FAR, MDR, and average sample number).

The remainder of this paper is organized as follows. The system model is given in Section II. The proposed scheme is given and analyzed mathematically with the Markov chain-based analytical model in Section III. The performance analysis is provided in Section IV, and the conclusion is drawn in Section V. Some important symbols used in this paper are listed in the following table.

Symbol	Description
n	Observation index.
N	Total number of active buses in the power system.
M	Total number of active power measurement data.
\mathbf{Z}	Set of power measurement data.
\mathbf{x}	Set of state.
\mathbf{e}	Set of measurement noise.
\mathbf{H}	Measurement Jacobian matrix.
\mathbf{B}	Network topology error matrix.
\mathcal{H}_e	Possible hypothesis, $e \in \{0, 1, 2, \dots\}$.
k	Repetition index for determining network topology.
\hat{h}	Prior probability of the hypothesis.
P_k	Posterior probability of the hypothesis.
c_e	Cost of falsely rejecting the hypothesis.
T	Minimum stopping time, $T \in n$.

II. SYSTEM MODEL

Before reviewing the classical formulation of the state estimation for the power network, we like to present the scope of smart grid state estimation as described in Fig. 1. In this figure,

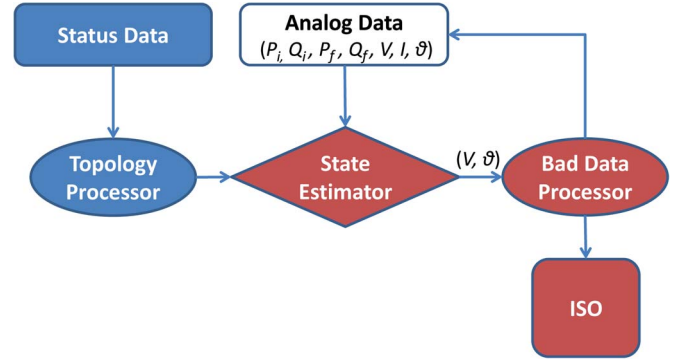


Fig. 1. Illustration of status data effect on the state estimation processor and further on the ISO. Analog data include the measurement data of power injection P_i , reactance injection Q_i , power flow P_f , reactance flow Q_f , bus voltage V , bus current I , and bus phase θ .

the network topology processor uses the telemetered data of the breaker and switch status to determine the present network topology of the system. Then, the state estimator processes both sets of measurement data (status and analog data) globally and takes advantage of its redundancy to detect any data error. If data error exists, a bad-data processor will notify the state estimator, and then, the estimated state of the power system will be discarded and reestimated again. Otherwise, the independent system operator (ISO) makes the decision for controlling generators and managing load by applying the current state into the different functions such as the automatic generation control, optimal power flow, or EMS. If the accident occurs, erroneous data can magnify the negative impact on these smart grid operations. Therefore, the efficient online error detection on measurement data is essential.

While the errors for analog data will cause the state estimation errors, the effect of topology error shall be analyzed to understand how it can be used for determining topology error. First, we consider the state estimation problem as estimating phase angles θ_q by observing the real-time measurements of active power flow. The initial phase angle θ_0 is known as reference angle, and therefore, only N angles have to be estimated. In other words, we have the total of N active angles (buses) in the system. The voltage level of each bus and reactance of each transmission line are assumed to be known.

A. Traditional BDD

We first review the classical formulation of the state estimation using the normal equations. At the observation index $n \in \{1, 2, 3, \dots\}$, the control center observes a vector \mathbf{Z}_n of M actual power measurements. The nonlinear equation relating the state vector \mathbf{x} is

$$\mathbf{Z}_n = \mathbf{h}(\mathbf{x}) + \mathbf{e}_n \quad (1)$$

where $\mathbf{Z}_n = [Z_{n,1}, \dots, Z_{n,M}]^T$ and \mathbf{e}_n is the Gaussian measurement noise with zero mean and covariance matrix Σ_e . By applying the Gauss–Newton method [17], the unknown state \mathbf{x} can be estimated iteratively as

$$\hat{\mathbf{x}}^{s+1} = \hat{\mathbf{x}}^s + (\mathbf{H}_s^T \Sigma_e^{-1} \mathbf{H}_s)^{-1} \mathbf{H}_s^T \Sigma_e^{-1} [\mathbf{Z}_n - \mathbf{h}(\hat{\mathbf{x}}^s)] \quad (2)$$

where the estimated system state $\hat{\mathbf{x}}^s \in \mathbb{R}^M$, s is the iteration number, and $\mathbf{H}_s \in \mathbb{R}^{M \times N}$ is the Jacobian evaluated at $\hat{\mathbf{x}}^s$

$$\mathbf{H}_s = \left. \frac{\partial \mathbf{h}(\hat{\mathbf{x}}^s)}{\partial \mathbf{x}} \right|_{\mathbf{x}=\hat{\mathbf{x}}^s}. \quad (3)$$

By decoupling the real and reactive part of measurements and state vectors, we will assume that the phase differences between two buses in the power network are all small. Then, a linear approximation of (1) is accurate, and we obtain

$$\mathbf{Z}_n = \mathbf{H}\mathbf{x} + \mathbf{e}_n \quad (4)$$

where \mathbf{Z}_n is the set of power measurements¹ (i.e., the power flow, power injection, or voltage), \mathbf{x} is the set of real part of $[\theta_1, \theta_2, \dots, \theta_{N-1}, \theta_N]^T$ (bus angles), and $\mathbf{H} \in \mathbb{R}^M$ is the measurement Jacobian matrix with respect to phase angles. As a result, the estimated state $\hat{\mathbf{x}}$ is

$$\hat{\mathbf{x}} = (\mathbf{H}^T \boldsymbol{\Sigma}_e^{-1} \mathbf{H})^{-1} \mathbf{H}^T \boldsymbol{\Sigma}_e^{-1} \mathbf{Z}_n. \quad (5)$$

For the bad-data detection (BDD) system, we compare the power-flow measurements \mathbf{Z}_n with the estimated active power flow $\hat{\mathbf{Z}}_n$ by the phase angle estimate $\hat{\mathbf{x}}$. $\hat{\mathbf{Z}}_n$ can be written as

$$\hat{\mathbf{Z}}_n = \mathbf{H}\hat{\mathbf{x}} = \mathbf{H} (\mathbf{H}^T \boldsymbol{\Sigma}_e^{-1} \mathbf{H})^{-1} \mathbf{H}^T \boldsymbol{\Sigma}_e^{-1} \mathbf{Z}_n = \mathfrak{S} \mathbf{Z}_n \quad (6)$$

where \mathfrak{S} is known as the *hat matrix*. Define the residue vector as

$$\mathbf{R}_n = \mathbf{Z}_n - \hat{\mathbf{Z}}_n. \quad (7)$$

The expected value and the covariance of residual \mathbf{R}_n are

$$E(\mathbf{R}_n) = \mathbf{0} \quad (8)$$

$$\boldsymbol{\Sigma}_{\mathbf{R}} = \left[\mathbf{I} - \mathbf{H} (\mathbf{H}^T \boldsymbol{\Sigma}_e^{-1} \mathbf{H})^{-1} \mathbf{H}^T \boldsymbol{\Sigma}_e^{-1} \right] \boldsymbol{\Sigma}_e \quad (9)$$

respectively. Generally, the bad \mathbf{Z}_n such as corrupted data, missed data, or topology error can typically trigger a BDD alarm since the measurement residual \mathbf{R}_n in (7) increases.

B. Topology Error

The effect of topology error can be presented in \mathbf{H} and effected on $E(\mathbf{R}_n)$, which is no longer to be zero. As mentioned in Section I, the system can perform BDD to determine the error by some comprehensive algorithms such as the sequential search algorithm, the chi-square test with weighted least squares state estimation, or the largest normalized residual test. Nevertheless, some of the known computational issues and shortcomings for these algorithms are explicitly described in [17]. From (4), the measurement of state estimation under the network topology error can be modeled in the following manner [19]:

$$\mathbf{H} = \mathbf{H}_e + \mathbf{B} \quad (10)$$

¹Each measurement has a different dimension, and the following study is based on power-flow estimation.

where \mathbf{H} is the true Jacobian measurement, \mathbf{H}_e is the incorrect Jacobian measurement due to topology errors, and \mathbf{B} is the Jacobian error matrix. Next, we substitute (10) into the linear approximation model (4) that yields

$$\mathbf{Z}_n = \mathbf{H}_e \mathbf{x} + \mathbf{B}\mathbf{x} + \mathbf{e}_n. \quad (11)$$

Next, the statistical characteristics of the new residual vector can be derived as follows. The residual under error with its covariance is

$$\mathbf{R}_n = \left[\mathbf{I} - \mathbf{H}_e (\mathbf{H}_e^T \boldsymbol{\Sigma}_e^{-1} \mathbf{H}_e)^{-1} \mathbf{H}_e^T \boldsymbol{\Sigma}_e^{-1} \right] [\mathbf{B}\mathbf{x} + \mathbf{e}_n] \quad (12)$$

$$\boldsymbol{\Sigma}_{\mathbf{R}} = \left[\mathbf{I} - \mathbf{H}_e (\mathbf{H}_e^T \boldsymbol{\Sigma}_e^{-1} \mathbf{H}_e)^{-1} \mathbf{H}_e^T \boldsymbol{\Sigma}_e^{-1} \right] \boldsymbol{\Sigma}_e \quad (13)$$

and the expected value of residual \mathbf{R}_n is

$$E(\mathbf{R}_n) = \left[\mathbf{I} - \mathbf{H}_e (\mathbf{H}_e^T \boldsymbol{\Sigma}_e^{-1} \mathbf{H}_e)^{-1} \mathbf{H}_e^T \boldsymbol{\Sigma}_e^{-1} \right] [\mathbf{B}\mathbf{x}]. \quad (14)$$

In other words, the ISO receives scramble measurement data and needs to identify/determine the erroneous status data that are generated by multiple buses in the power grid network. This type of problem can also be seen as the detection problem for dealing with the demodulation of the mutually interfering digital streams of information.

C. Problem Formulation

In fact, we can consider each bus in smart grid networks as a single transmitter through a common communication channel that carries the information such as the network topology. Let us first consider the expanded version of (4) that yields

$$\begin{pmatrix} Z_{n,1} \\ Z_{n,2} \\ \vdots \\ Z_{n,M} \end{pmatrix} = \begin{pmatrix} H_{1,1} & \cdots & H_{1,N} \\ H_{2,1} & \cdots & H_{2,N} \\ \vdots & \ddots & \vdots \\ H_{M,1} & \cdots & H_{M,N} \end{pmatrix} \begin{pmatrix} x_1 \\ x_2 \\ \vdots \\ x_N \end{pmatrix} + \begin{pmatrix} e_{n,1} \\ e_{n,2} \\ \vdots \\ e_{n,M} \end{pmatrix}. \quad (15)$$

In contrast, we can also describe the power measurement matrix of (15) in the formulation of the sequential process; for the representation of the entire power grid network, each power measurement information \mathbf{Z}_n can be expressed as

$$\begin{aligned} Z_{n,1} &= \sum_{i=1}^N H_{1,i} \hat{x}_i + e_{n,1} \\ Z_{n,2} &= \sum_{i=1}^N H_{2,i} \hat{x}_i + e_{n,2} \\ &\vdots \\ Z_{n,r} &= \sum_{i=1}^N H_{r,i} \hat{x}_i + e_{n,r} \\ &\vdots \\ Z_{n,M-1} &= \sum_{i=1}^N H_{M-1,i} \hat{x}_i + e_{n,M-1} \\ Z_{n,M} &= \sum_{i=1}^N H_{M,i} \hat{x}_i + e_{n,M} \end{aligned} \quad (16)$$

where the row $r \in \{1, 2, \dots, M\}$ and the measurement noise is $e_{n,r}$ at r .

The idea is to enable several buses to send information simultaneously through a communication channel; on the control center, the noisy version of the superposition of signals is obtained from a crowd of the active buses, and next, the operator works an efficient way to decode and estimate the useful information that is sent by the individual buses. We like to online estimate \mathbf{H} with minimal delay in order to help one compute \mathbf{B} and \mathbf{H}_e and further identify the topology error efficiently. Thus, the main task is how to estimate each element of \mathbf{H} as quickly as possible with a certain level of error probability, i.e.,

$$\min k, \text{ s.t. } P_r(\mathbf{H} \neq \hat{\mathbf{H}}) \leq \eta \quad (17)$$

where k represents the index of each repetition, $\hat{\mathbf{H}}$ is the estimated measurement Jacobian matrix, and η is a certain threshold of error probability. We assume that the errors in status data of breakers and switches result in the erroneous assertion of the network topology in terms of branch outage, bus split, or shunt capacitor/reactor switching. At ISO, the true measurement Jacobian matrix is already determined. After a short period of time, the topology error occurs in the network. Our objective is to determine the present measurement Jacobian matrix under topology errors with as little delay as possible so as to help compute the resulting error matrix \mathbf{B} and \mathbf{H}_e efficiently to identify the problem. In other words, the present network topology is sequentially estimated with the minimal delay.

III. PROPOSED SCHEME

In this section, we investigate one type of the detection/estimation mechanisms against topology error in the smart grid. In brief, we have developed a novel estimation strategy via an online statistical analysis of a sequence of data, which can control the detection delay and error probability under the desired levels. The conventional state estimation methods [18] for BDD use measurements to balance the FAR and the missing detection rate, while our approach aims to minimize the detection delay under the error probability constraint.

The proposed scheme, the *adaptive quickest estimation algorithm*, is the modification of the classic sequential probability ratio test [12]. To estimate the network topology efficiently based on the observed measurements, the proposed scheme contains two interleaved steps that are computed iteratively until the completion of $\hat{\mathbf{H}}$. With such information, ISO can explicitly determine topology error matrix \mathbf{B} via comparing \mathbf{H} . Note that we also develop an analytical model based on the Markov chain, which provide a guidance to configure the detection system for performance guarantee. In this section, we first give the overview of the proposed quickest estimation algorithm. Details of the proposed algorithm are then described and analyzed with a Markov chain-based model.

A. Overview

There are many ways to express the network topology [18], [17]. The network topology is also known as the measurement

Jacobian matrix \mathbf{H} . In the matrix, an element $H_{r,i}$ can take the values from set $\{1, -1, 0\}$, respectively, with 1 indicating the power flow from bus a to bus b , -1 indicating the power flow from the bus b to bus a , or 0 indicating the ‘‘off’’ switch status between the two buses. If the erroneous status data occur in the network, then on–off statuses may be exchanged. Note that the ‘‘off’’ status under the error may become the active power measurement with either the positive or negative direction.

In a general step, we assume that $\vec{\mathbf{H}}_1, \dots, \vec{\mathbf{H}}_{r-1}$ have been already estimated. The proposed scheme works as follows:

- 1) The true \mathbf{H} with true $\vec{\mathbf{H}}_r$ removed is used to estimate $\hat{\mathbf{x}}$ by (5) beforehand, which is then further used to estimate the Jacobian matrix under possible topology errors, i.e., $\hat{\mathbf{H}}$. This step is to ensure the calculation accuracy of $\hat{\mathbf{H}}_r$ in later steps. As the number of measurements $M \gg N$, removing one measurement will not impact the accuracy in estimating $\hat{\mathbf{x}}$.
- 2) Consider \mathbf{Z}_n in the multiple access format as in (16). Given $\vec{\mathbf{H}}_1, \dots, \vec{\mathbf{H}}_{r-1}$, $Z_{n,r}$ will be modified as $Z'_{n,r} = Z_{n,r} - \sum_{i=0}^{r-1} \hat{x}_i \hat{H}_{r,i}$. $Z'_{n,r}$ will be used to estimate $\vec{\mathbf{H}}_r$.
- 3) The elements of $\vec{\mathbf{H}}_r$ will be estimated with an iterative algorithm, which is to be discussed in detail later.
- 4) With $\vec{\mathbf{H}}_r$ obtained, go back to *Stage 1*, and update $r = r + 1$. The algorithm ends when the $\hat{\mathbf{H}}$ is fully constructed.

B. Proposed Methodology

After removing previous measurements related to $\vec{\mathbf{H}}_1, \dots, \vec{\mathbf{H}}_{r-1}$ in *Stage 1*, $Z'_{n,r}$ of *Stage 2* is then used to estimate $\vec{\mathbf{H}}_r$ with two interleaved steps in *Stage 3* in Section III-A.

1) *Step 1—Statistical Hypothesis Test*: Next, to solve each $H_{r,i}$, we expand each power measurement to the continuous-time sequence as shown (16). With $Z_{n,r}$ updated to $Z'_{n,r}$ as described in *Stage 2* in Section III-A, the present measurement can be implicitly described as

$$Z'_{n,r} = \hat{x}_i H_{r,i} + e_{n,r} \quad (18)$$

with the items related with $i \in \{r+1, \dots, N\}$ merging into $e_{n,r}$ as the background noise (sum of interference and measurement noise). Without loss of generality, $Z'_{n,r}$ can be composed by three possible statistical hypotheses ($\mathcal{H}_0, \mathcal{H}_1, \mathcal{H}_2$) of

$$\begin{cases} \mathcal{H}_0 : Z'_{n,r} \sim \mathcal{N}(-\hat{x}_r, \sigma_r^2) \\ \mathcal{H}_1 : Z'_{n,r} \sim \mathcal{N}(0, \sigma_r^2) \\ \mathcal{H}_2 : Z'_{n,r} \sim \mathcal{N}(\hat{x}_r, \sigma_r^2) \end{cases} \quad (19)$$

where σ_e^{22} plus the interference of the rest of the items has the power of

$$\sigma_r^2 = \sigma_e^2 + \sum_{j=r+1}^N (\hat{x}_j)^2. \quad (20)$$

To sequentially estimate each $H_{r,i}$ in (18) correctly, three possible combinations of binary hypothesis test are considered,

²In the case of items with $H_{r,i} = 0$, the σ_e^2 is equivalent to σ_r^2 .

namely

$$\hat{H}_{r,i} = \begin{cases} \text{Test 1 : } \mathcal{H}_0 & \text{vs. } \mathcal{H}_1 \\ \text{Test 2 : } \mathcal{H}_1 & \text{vs. } \mathcal{H}_2 \\ \text{Test 3 : } \mathcal{H}_2 & \text{vs. } \mathcal{H}_1 \end{cases} \quad (21)$$

where $\hat{H}_{r,i}$ is the estimated value of $H_{r,i}$. Now, we can formulate the quickest estimation problem for each test in (21), and the procedure is described hereinafter in generalized term of the hypothesis test: $\tilde{\mathcal{H}}_0$ versus $\tilde{\mathcal{H}}_1$. Therefore, we like to make a decision between these hypotheses in a way of minimizing an appropriate measure of error probability and cost.

2) *Step 2—Sequential Decision Problem:* Let $(1 - \tilde{h})$ represent the prior probability of $\tilde{\mathcal{H}}_0$ and \tilde{h} represent the prior probability of $\tilde{\mathcal{H}}_1$. Based on [12], we can formulate the posterior probability P_k of $\tilde{\mathcal{H}}_1$ with a sequence of $Z_{n,r}^k$ in present

$$P_k = \frac{\tilde{h} \prod_{i=1}^k f_1(Z_{n,r}^i)}{\tilde{h} \prod_{i=1}^k f_1(Z_{n,r}^i) + (1 - \tilde{h}) \prod_{i=1}^k f_0(Z_{n,r}^i)} \quad (22)$$

where $f_1(\cdot)$ is the probability density function of $\tilde{\mathcal{H}}_1$ and $f_0(\cdot)$ is the probability density function of $\tilde{\mathcal{H}}_0$. By the recursion, the posterior probability P_k of $\tilde{\mathcal{H}}_1$ can be rewritten as

$$P_k = \frac{P_{k-1} f_1(Z_{n,r}^k)}{P_{k-1} f_1(Z_{n,r}^k) + (1 - P_{k-1}) f_0(Z_{n,r}^k)} \quad (23)$$

where the initial value P_1 is equal to \tilde{h} . We now can recursively determine P_k in real time. The constraint function for the decision threshold shall be defined as well so that the system can know whether $\tilde{\mathcal{H}}_1$ or $\tilde{\mathcal{H}}_0$ is the true hypothesis.

The estimation constraint c_e with the error probability cost for the decision rule is formulated as

$$c_e = c_0(1 - \tilde{h})\alpha + c_1\tilde{h}\beta \quad (24)$$

and the terminal decision is

$$\mathcal{D}_k = \begin{cases} 1, & P_k \geq \frac{c_0}{c_0 + c_1} \\ 0, & P_k < \frac{c_0}{c_0 + c_1} \end{cases} \quad (25)$$

where $c_j > 0, j \in (0, 1)$, is the cost of falsely rejecting \hat{H}_j , α is $P_0(\mathcal{D}_k = 1)$ known as the FAR, and β is $P_1(\mathcal{D}_k = 0)$ known as the MDR. If the posterior probability is greater than or equal to the threshold, $\tilde{\mathcal{H}}_1$ is declared ($\mathcal{D}_k = 1$) as the true hypothesis; otherwise, $\tilde{\mathcal{H}}_0$ is declared ($\mathcal{D}_k = 0$). For the better estimation accuracy, we are able to reevaluate c_e by incorporating the Bayes optimal sequential decision rule based on [12] which can be rewritten as

$$C_v(P_v) = \min \{ \min [c_1 P_{v-1}, c_0(1 - P_{v-1})], C_{v-1}(P_{v-1}) \} \quad (26)$$

where $C_0(P_0) = \min [c_1 \tilde{h}, c_0(1 - \tilde{h})]$ and $v \in \{1, 2, \dots, V\}$ (V is the length of the training sequence). Note that the training sequence is needed for the computation of the new cost function C_v before the likelihood test can be executed. By incorporating both cost function vector \mathbf{C} and posterior vector \mathbf{P} , we can determine the minimum upper bound posterior probability P_U^{\min}

and maximum lower bound posterior probability P_L^{\max} of P_k as follows:

$$\begin{cases} P_L^{\max} = \max[0 \leq \mathbf{P} \leq \tilde{h} | \mathbf{C} = c_1 \mathbf{P}] \\ P_U^{\min} = \min[\tilde{h} \leq \mathbf{P} \leq 1 | \mathbf{C} = c_0(1 - \mathbf{P})]. \end{cases} \quad (27)$$

With the similar formulation of (25), the threshold of accepting $\tilde{\mathcal{H}}_0$ in terms of P_U^{\min} and P_L^{\max} can be described as

$$A = \frac{1 - \tilde{h}}{\tilde{h}} \frac{P_L^{\max}}{1 - P_L^{\max}} \quad (28)$$

and the threshold of accepting $\tilde{\mathcal{H}}_1$ is

$$B = \frac{1 - \tilde{h}}{\tilde{h}} \frac{P_U^{\min}}{1 - P_U^{\min}}. \quad (29)$$

Finally, the minimal stopping time T of our proposed scheme with the Bayes optimal sequential decision rule can be written as

$$T = \inf \{k \geq 1 | \Lambda_k \ni (A, B)\} \quad (30)$$

where Λ_k is the sequence of the likelihood ratios

$$\Lambda_k = \frac{f_1(Z_{n,r}^k)}{f_0(Z_{n,r}^k)} \Lambda_{k-1} \quad (31)$$

with the initial value of $\Lambda_0 = 1$ at time interval $k = 0$. A decision is made at each interval k to whether continue sampling or terminate the test and declare the true hypothesis. If Λ_k either exceeds the threshold B (to declare that the true hypothesis is $\tilde{\mathcal{H}}_1$) or is less than the threshold A (to declare that the true hypothesis is $\tilde{\mathcal{H}}_0$), the hypothesis decision is made, and the process is terminated. Now, we want to decode the element of \mathbf{H} of bus $i + 1$. By the source separation method, $\hat{x}_i \hat{H}_{r,i}$ is now eliminated from the sequence of the observation. The newly updated sequence of observation is as follows:

$$Z_{n,r}^k = Z_{n,r}^k - \hat{x}_i \hat{H}_{r,i} \quad (32)$$

where $\hat{H}_{r,i}$ denotes the estimation of $H_{r,i}$. *Stage 3* is terminated until the completion of estimating $\vec{\mathbf{H}}_r$.

At *Stage 4*, we update the next available measurement ($Z_{n,r+1}$) and $\vec{\mathbf{H}}_r = \vec{\mathbf{H}}_{r+1}$. Then, we return *Stage 1* and repeat the stages from the beginning of this section until recovering the last element $\hat{H}_{M,N}$ of \mathbf{H} . In other words, the $\hat{\mathbf{H}}$ is fully constructed. Note that a summary of the proposed scheme is shown in Algorithm 1.

C. Mathematical Analysis

In this section, we develop the Markov chain-based analytical model to systematically examine the proposed scheme. The Markov chain-based analytical model produces the quantitative performance analysis and theoretical guidance on the proposed scheme's parameter configuration for performance guarantee under fundamental performance metrics: the expectation of FAR and the expectation of MDR.

Algorithm 1 Adaptive Quickest Estimation for $\hat{\mathbf{H}}$

known $\hat{\mathbf{x}}$
repeat
 unknown $\vec{\mathbf{H}}_r$
 repeat
 unknown $H_{r,i}$ in (18)
 repeat
 compute the posterior probability P_k
 the training sequence:
 for $v = 1$ to V **do**
 compute the cost function, $C_v(P_v)$, and $v \leftarrow v + 1$
 end for
 Threshold calculation:
 compute the boundary posterior probabilities $\{P_L^{\max}, P_U^{\min}\}$, respectively, in (27)
 compute the boundary thresholds A and B
 Likelihood test:
 compute Λ_k
 Update of: $k \leftarrow k + 1$
 continue the observation
 until $T = \inf\{k \geq 1 | \Lambda_k \ni (A, B)\}$ in (31)
 report the true hypothesis and store $\hat{H}_{r,i}$
 update $Z_{n,r}$ via removing $\hat{x}_i \hat{H}_{r,i}$ in (32)
 update $H_{r,i} = H_{r,i+1}$,
 until completion of estimating $\vec{\mathbf{H}}_r$
 update $Z_{n,r} = Z_{n,r+1}$, and $\vec{\mathbf{H}}_r = \vec{\mathbf{H}}_{r+1}$
 until completion of estimating $\hat{\mathbf{H}}$

1) Analysis Model: For analysis purpose, we discretize $\mathbb{R}^+ \cup 0$ into the finite sets $\{U_1, \dots, U_{F-1}, U_F\}$, where $U_1 = 0$ and U_F is the set whose value is greater than or equal to h . In other words, F is the total number of transitions from 0 to the state that has the value greater than or equal to h . There are several approaches for discretization [20], [21]. In this paper, we employ uniform sampling for simplicity.³ Moreover, from (31), we know that the sequence exhibits the Markov property, where the current state $j = \Lambda_k$ at observation k only depends on the previous state $i = \Lambda_{k-1}$ at $k - 1$, but not on the past history [22].

The transition probabilities of the Markov chain for the proposed scheme from state i at $(k - 1)$ to state j at k can be described as

$$\begin{aligned}
 P_{ij} &= P[\Lambda_k = j | \Lambda_{k-1} = i], \text{ under } \tilde{H}_0; \\
 \hat{P}_{ij} &= P[\Lambda_k = j | \Lambda_{k-1} = i], \text{ under } \tilde{H}_1.
 \end{aligned} \quad (33)$$

We can calculate the TPMs \mathbf{P} and $\hat{\mathbf{P}}$, with the size of $(F + 1) \times (F + 1)$, under the hypothesis \tilde{H}_0 and \tilde{H}_1 according to $f_0(Z_{n,r}^k)$ and $f_1(Z_{n,r}^k)$, respectively.

The initial steady-state probability of the Markov chain, where the process starts from a normal state, can be determined as

$$\pi_j^0 = \frac{\pi_j}{\sum_{i=0}^{F-1} \pi_i}, \text{ given } j \in \{0, U_1, \dots, U_{F-1}\} \quad (34)$$

³Other discretization methods can be employed like the μ -law or A-law in pulse-code modulation.

and the steady-state probability can be determined

$$\pi_j = \sum_{i=0}^F P_{ij} \pi_i \quad (35)$$

where $j \in \{0, U_1, \dots, U_F\}$ and $\sum_{j=0}^F \pi_j = 1$.

2) Expectation of FAR: Next, based on the Markov chain model, we study the theoretical performance analysis of FAR and MDR expectations, respectively. The expectation ($E_{\mathbf{P}}[\text{FAR}]$) of the FAR is the probability that the proposed statistic Λ_k reaches to the state U_F when the hypothesis \tilde{H}_0 is true. According to Gamerman and Lopes [22], the TPM \mathbf{P} always has a special eigenvector with only one eigenvalue $\lambda = 1$, and the rest are zero. Thus, we can obtain the solution by re-elaborating (35) into the matrix form as

$$\begin{bmatrix} P_{00} - 1 & P_{01} & \cdots & P_{0F} \\ P_{10} & P_{11} - 1 & \cdots & P_{1F} \\ \vdots & \vdots & \ddots & \vdots \\ P_{F0} & P_{F1} & \cdots & P_{FF} - 1 \\ 1 & 1 & \cdots & 1 \end{bmatrix} \begin{bmatrix} \pi_0 \\ \pi_1 \\ \vdots \\ \pi_F \end{bmatrix} = \begin{bmatrix} 0 \\ 0 \\ \vdots \\ 0 \\ 1 \end{bmatrix}. \quad (36)$$

Then, the expectation of FAR can be determined by

$$E_{\mathbf{P}}[\text{FAR}] = \pi_F. \quad (37)$$

3) Expectation of MDR: We define the missed detection probability (MDP) as the probability that the detection delay is greater than or equal to a detection delay constraint C . The expectation ($E_{\hat{\mathbf{P}}}[\text{MDR}]$) of the MDP is, starting from the initial state, the summation of probabilities that Λ_k stays at a state other than state U_F at time C . Let $p_i(s)$ denote the probability of the state variable at time s and at state i . We set the initial condition for the transition probabilities as

$$p_i(0) = \pi_i^0 \quad (38)$$

where $i \in \{0, U_1, \dots, U_{F-1}\}$ and $p_F(0) = 0$. By the iteration, at each s , the state probability vector is updated by the previous state probability vector in a matrix form as

$$\begin{bmatrix} p_0(s) \\ p_1(s) \\ \vdots \\ p_{F-1}(s) \\ p_F(s) \end{bmatrix}^T = \begin{bmatrix} p_0(s-1) \\ p_1(s-1) \\ \vdots \\ p_{F-1}(s-1) \\ p_F(s-1) \end{bmatrix}^T \hat{\mathbf{P}} \quad (39)$$

$$p_F(s) = 0, \quad s \in \{0, C - 1\}. \quad (40)$$

Here, the $p_F(s)$ at every s of state U_F is reset to zero for the next iteration since we are only concerned with the missed detection case. The expectation of MDR under the given delay constraint C can be obtained as

$$E_{\hat{\mathbf{P}}}[\text{MDR}] = \sum_{i=0}^{F-1} p_i(C). \quad (41)$$

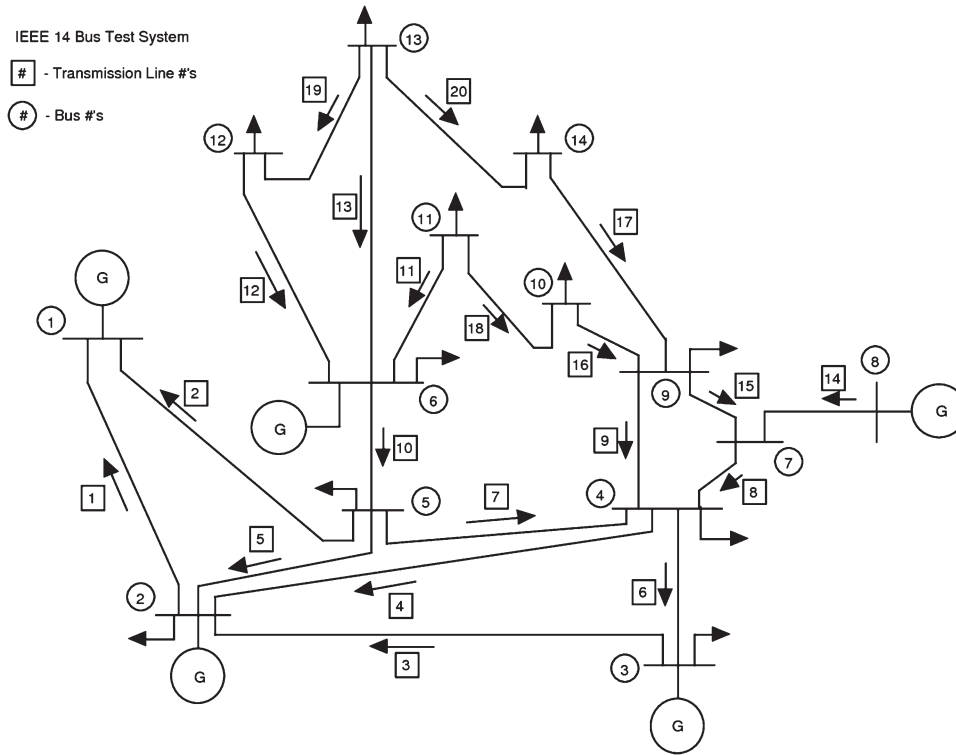


Fig. 2. Schematic graph of IEEE 14-bus test system with five generators (G).

IV. PERFORMANCE ANALYSIS

In this section, we use both analytical and numerical simulations to demonstrate the performance of the proposed scheme by MATPOWER 4.0 package [23]. MATPOWER 4.0 provides realistic power flow data and test systems that are used widely in research-oriented study. All simulations are performed under the IEEE 14-bus test system as shown in Fig. 2, which has five generators for 20 measurements; the arrow represents the power-flow directions, and the triangular (attached on the bus) is the load. Note that we first apply the analytical model to theoretically analyze the performance of the detection system for guiding the system parameter configuration. Next, we use the parameter from the theoretical analysis to confirm the accuracy of the analysis, and then, we demonstrate the performance of the detection.

Fig. 3 shows an illustrative example of decoding/estimating $H_{r,i}$ of bus i . The dot represents Λ_k , and \hat{h} is set to 0.5 with the maximum cost constraint. The simulation result shows that the threshold A is 0.017 and the threshold B is 92. From Fig. 3, the decision is declared at minimum stopping time T which is 12 after falling under the threshold A , and the value of $\hat{H}_{r,i}$ is -1 in this case.

The numerical examination is presented in Fig. 4 for understanding the impact of average sample number (ASN) on system parameters c_0 and c_1 of the proposed scheme. Note that the x -axis is the bus index and the y -axis is the corresponding ASN for each bus. There are three settings: 1) the low cost with $c_0 = 1$ and $c_1 = 2$; 2) the median cost with $c_0 = 3$ and $c_1 = 4$; and 3) the high cost with $c_0 = 6$ and $c_1 = 8$. As shown in the figure, the higher cost of falsely rejecting the hypothesis causes larger ASN (i.e., the system needs to spend more observations

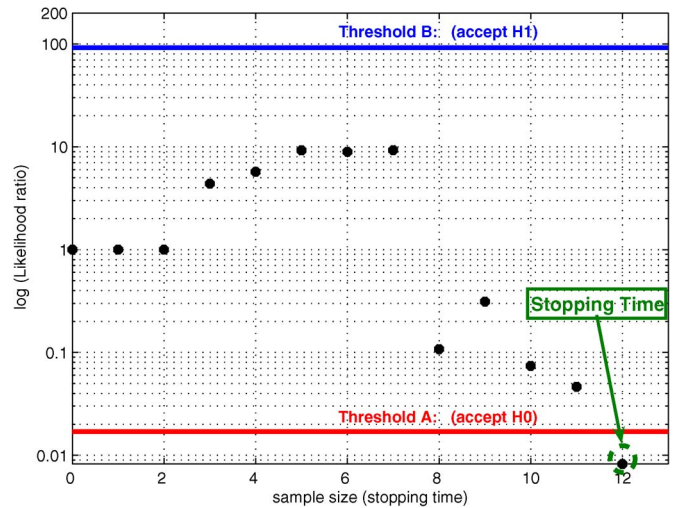


Fig. 3. Simulation of the proposed scheme in QD for determining $H_{r,i}$ of the bus i under an IEEE 14-bus test system.

for making a decision). In other words, the higher cost setting may result in the better estimation accuracy but have the longer decision delay.

As shown in both Figs. 5 and in 6, the analytical performance measures and the simulation results are compared under the same setting and input data for the examination. By using power flow data sets from MATPOWER 4.0, the performance index ($E[FAR]$, $E[MDR]$) comparisons between the analytical and simulation results can be conducted. With the parameter from the theoretical analysis, the performance indices are simulated (both theoretical analysis and simulation are plotted respectively to confirm the accuracy of

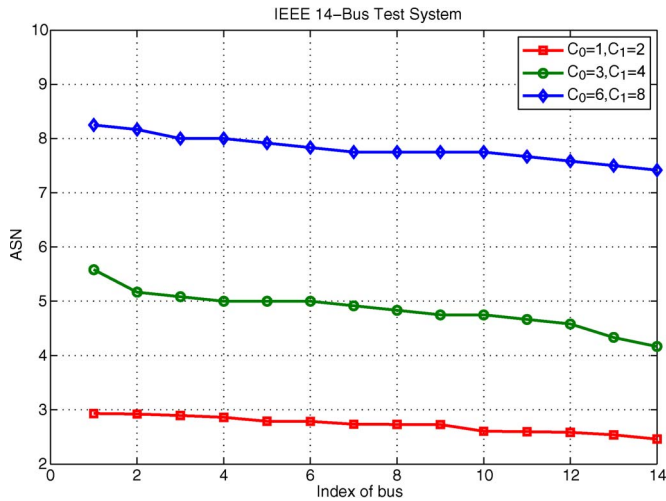


Fig. 4. ASN under three sets of error cost scenarios for IEEE 14-bus test system.

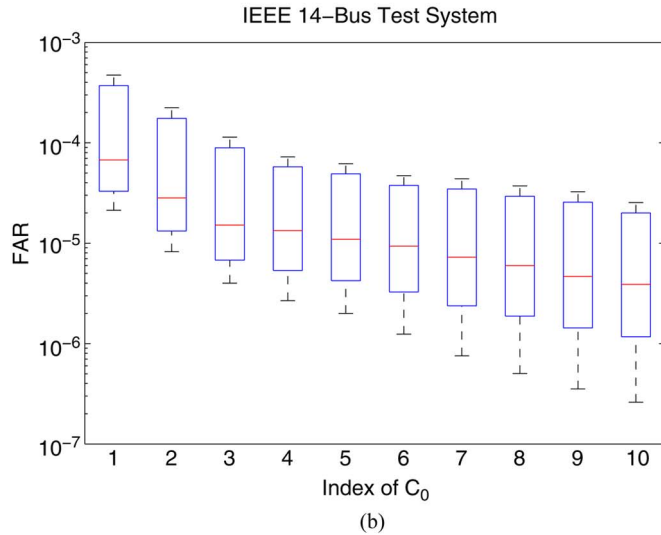
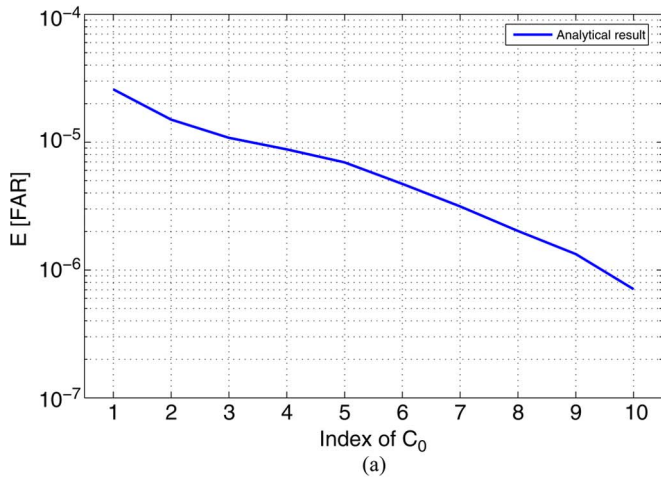


Fig. 5. Comparison between the analytical and numerical results under $c_1 = 1$ for the IEEE 14-bus test system. (a) Expectation of FAR via Markov chain-based analytical model. (b) FAR via numerical simulation.

analysis and demonstrate the performance) so that we can properly configure the proposed algorithm for the guaranteed performance.

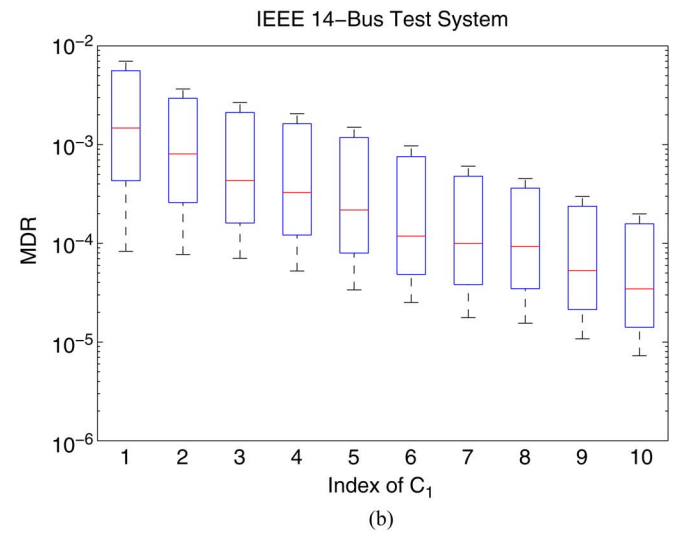
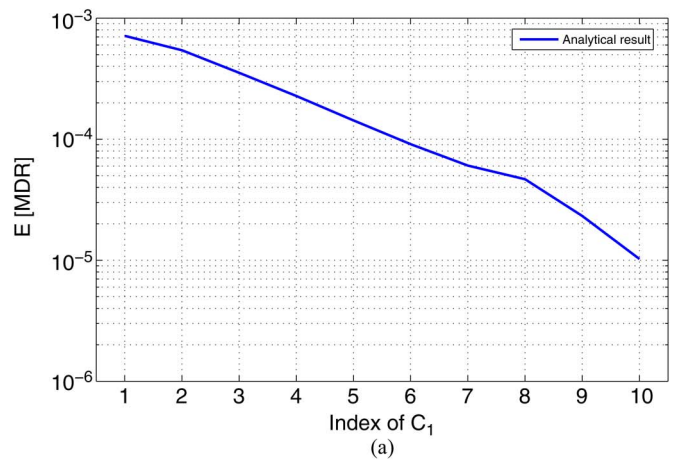


Fig. 6. Comparison between the analytical and numerical results under $c_0 = 1$ for the IEEE 14-bus test system. (a) Expectation of MDR via Markov chain-based analytical model. (b) MDR via numerical simulation.

Fig. 5 illustrates the relation between the system parameter c_0 and performance metrics (FAR). Note that the logarithmic scale is used in the figure for the vertical axis. FAR is computed via applying c_0 from 1 to 10 in the ascending order, while retaining the value of c_1 to 1 (i.e., c_0 is the cost of falsely rejecting \hat{H}_0). As shown in Fig. 5, the analytical and simulation results are fairly close. Fig. 5(a) is the result of the Markov chain-based analytical model of the proposed scheme. In Fig. 5(b), the central mark is the median, and the edges of the box are the 25th and 75th percentiles. The whiskers extend to the most extreme data points (the maximum and minimum values of FAR). The maximum value of FAR is close to the edge of the box; it means that the worst case for each set is not far away from the majority value of FAR. The difference percentage between the median and the maximum FAR is about 8%, but smaller FAR is always desired in this simulation. To compare with Fig. 5(a) and (b), the analytical FAR usually falls right on or slightly below the 25th percentile edge of the box, but it never exits the minimum FAR of the numerical result. In other words, the analytical model gives us a more ideal/theoretical value of FAR for the proposed algorithm that is less than the median FAR of the numerical result. From

Fig. 5, we also observe that a larger c_0 yields a smaller FAR as expected.

The result is shown in Fig. 6 that helps us study the impact of the MDR on c_1 of the proposed scheme (i.e., c_1 is the cost of falsely rejecting \hat{H}_0). Note that the logarithmic scale is used in the figure for the vertical axis. MDR is computed via applying c_1 from 1 to 10 in the ascending order, and the value of c_0 is equal to 1 through the process. Fig. 6(a) is the expectation of MDR under the detection delay constraint of the Markov chain-based model. As presented in Fig. 6(b), the center mark is the median of MDR, and the edges of the rectangle are the 25th and 75th percentiles. The whiskers extend to the maximum and minimum values of MDR, respectively. The maximum MDR of each set is much close to the majority of MDR in comparison to the minimum MDR; the smaller the worst case of MDR, the better the performance. In Fig. 6(a) and (b), we observe that the value of analytical MDRs falls on the region between the 25th percentile and median MDR of numerical simulation; in other words, the median MDR of the numerical result is fairly close to the analytical results. The detection delay constraint, which is introduced in the formulation of calculating analytical MDR, may give additional reinforcement on the simulation accuracy. From Fig. 6, both analytical and numerical simulations show that the larger constraint c_1 results in smaller MDR as expected. In other words, the probability of true estimation rises if we allow to increase the cost of longer delay.

From Figs. 5 and 6, we demonstrate the performance metrics with different h . It also helps us configure the system parameters c_1 and c_0 for the guaranteed performance under fundamental metrics. We can select the proper configuration of $[c_1, c_0]$ from the reasonable range to satisfy the desired performance constraints. For example, in the low-cost configuration (i.e., the low-cost setting: both $c_0 = 1$ and $c_1 = 1$), one can explicitly determine the expectational FAR of 0.0005 and the expectational MDR of 0.007. In other words, the guarantee performance of the proposed algorithm is able to estimate the \mathbf{H} with minimal delay while maintaining comparable low error rates.

Finally, we consider that the performance of the proposed scheme in terms of the computational complexity. Since the proposed scheme heavily involves with the hypothesis testing, we like to understand the difference of computation time between the proposed scheme and the conventional hypothesis test algorithm [24]–[26]. The *size of an instance* is set to the number of cycles, which is used to compute ASN. The computational time is simulated by increasing the number of cycles. From Fig. 7, the computational time of the proposed scheme is much smaller than that of the conventional algorithm. Although the performances of both algorithms seem to linearly increase with the number of cycles for calculating ASN, the proposed method runs with 70% less computational time than that of the conventional algorithm.

V. CONCLUSION

In this paper, the main objective is to perform online estimation for the present network topology with minimal delay, in order to help detect and identify the topological error efficiently in smart grid networks. The proposed scheme, the *adaptive*

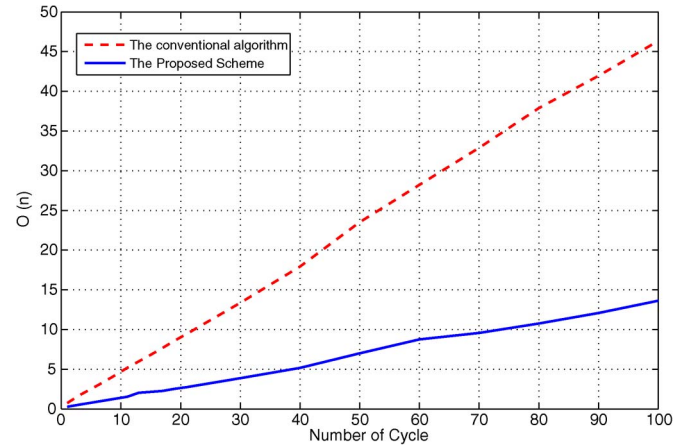


Fig. 7. Performance comparison of computational complexity by varying the number of ASN calculation cycles.

quickest estimation algorithm, successfully determines the current network topology as quickly as possible without violating the given constraints such as a certain level of estimation accuracy. As the present topology is solved, the operator can quickly determine and identify the network topology error timely. Furthermore, we are able to develop the Markov chain-based analytical model to characterize the behavior of our proposed scheme; one can quantitatively study the system parameters to achieve the guaranteed detection performance in terms of fundamental metrics. With the aid of the MATPOWER 4.0 package, both the analytical and numerical simulations are conducted under the simulated power test system to ensure the accuracy and proficiency; the simulation results have shown that the proposed scheme is efficient in terms of detection accuracy and minimum detection delay. The guaranteed performance of the proposed scheme under the low-cost scenario can be explicitly determined in terms of FAR and MDR, and the quickest estimation of the proposed algorithm is much efficient than the conventional scheme in terms of computational complexity.

REFERENCES

- [1] *The Smart Grid: An Introduction*, U.S. Department of Energy (DOE), Washington, DC, USA, Sep. 2010.
- [2] Y. Huang, L. Lai, H. Li, W. Chen, and Z. Han, "Online quickest multiarmed bandit algorithm for distributive renewable energy resources," in *Proc. IEEE Conf. Smart Grid Commun.*, Tainan, Taiwan, Nov. 2012, pp. 558–563.
- [3] A. M. Sasson, S. T. Ehrmann, P. Lynch, and L. S. Van Slyck, "Automatic power system network topology determination," *IEEE Trans. Power App. Syst.*, vol. PAS-92, no. 1, pp. 610–618, Mar. 1973.
- [4] T. E. DyLiacco, K. A. Ramaro, and A. W. Weiner, "Network status analysis for real-time systems," in *Proc. 8th PICA Conf.*, Jul. 1973, pp. 356–362.
- [5] P. Bonanomi and G. Gramberg, "Power system data validation and state calculation by network search techniques," *IEEE Trans. Power App. Syst.*, vol. PAS-102, no. 1, pp. 238–249, Jan. 1983.
- [6] R. L. Lugtu, D. F. Hackett, K. C. Liu, and D. D. Might, "Power system state estimation: Detection of topological errors," *IEEE Trans. Power App. Syst.*, vol. 99, no. 6, pp. 2406–2412, Nov. 1980.
- [7] J. Lin and H. Pan, "A static state estimation approach including bad data detection and identification in power systems," in *Proc. IEEE Power Eng. Soc. Gen. Meeting*, Tampa, FL, USA, Jul. 2007, pp. 1–7.
- [8] J. Chen and A. Abur, "Placement of PMUs to enable bad data detection in state estimation," *IEEE Trans. Power Syst.*, vol. 21, no. 4, pp. 1608–1615, Nov. 2006.

- [9] D. He, C. Chen, S. Chan, Y. Zhang, J. Bu, and M. Guizani, "Secure service provision in smart grid communication," *IEEE Commun. Mag.*, vol. 50, no. 8, pp. 53–61, Aug. 2012.
- [10] Y. Zhang, R. Yu, M. Nekovee, Y. Liu, S. Xie, and S. Gjessing, "Cognitive machine-to-machine communications: Visions and potentials for the smart grid," *IEEE Netw. Mag.*, vol. 26, no. 3, pp. 6–13, May/Jun. 2012.
- [11] Y. Huang, M. Esmalifalak, H. Nguyen, R. Zheng, Z. Han, H. Li, and L. Song, "Bad data injection in smart grid: Attack and defense mechanisms," *IEEE Commun. Mag.*, vol. 51, no. 3, pp. 27–33, Jan. 2013.
- [12] H. V. Poor and Q. Hadjiladis, *Quickest Detection*. Cambridge, U.K.: Cambridge Univ. Press, 2008.
- [13] Y. Huang, H. Li, K. A. Campbell, and Z. Han, "Defending false data injection attack on smart grid network using adaptive CUSUM test," in *Proc. Conf. Inf. Sci. Syst.*, Baltimore, MD, USA, Mar. 2011, pp. 1–6.
- [14] H. Li, C. Li, and H. Dai, "Quickest spectrum sensing in cognitive radio," in *Proc. 42nd Annu. Conf. Inf. Sci. Syst.*, Princeton, NJ, USA, Mar. 2008, pp. 203–208.
- [15] J. Tang, Y. Cheng, and W. Zhuang, "An analytical approach to real-time misbehavior detection in IEEE 802.11 based wireless networks," in *Proc. IEEE Int. Conf. Comput. Commun.*, Shanghai, China, Apr. 10–15, 2011, pp. 1638–1646.
- [16] M. Basseville and I. Nikiforov, *Detection of Abrupt Changes: Theory and Applications*. Englewood Cliffs, NJ, USA: Prentice-Hall, 1993.
- [17] A. Abur and A. G. Exposito, *Power System State Estimation: Theory and Implementation*. New York, NY, USA: Marcel Dekker, 2004.
- [18] A. Monticelli, *State Estimation in Electric Power Systems: A Generalized Approach (Power Electronics and Power Systems)*. New York, NY, USA: Springer-Verlag, May 1999.
- [19] F. F. Wu and W. R. Liu, "Detection of topology errors by state estimation," *IEEE Trans. Power Syst.*, vol. 4, no. 1, pp. 176–183, Feb. 1989.
- [20] M. R. Chmielewski and J. W. Grzymala-Busse, "Global discretization of continuous attributes as preprocessing for machine learning," *Int. J. Approx. Reason.*, vol. 15, no. 4, pp. 319–331, Nov. 1996.
- [21] Y. Q. Chen and K. L. Moore, "Discretization schemes for fractional-order differentiators and integrators," *IEEE Trans. Circuits Syst. I, Fundam. Theory Appl.*, vol. 49, no. 3, pp. 363–367, Mar. 2002.
- [22] D. Gamerman and H. F. Lopes, *Markov Chain Monte Carlo: Stochastic Simulation for Bayesian Inference*. Boca Raton, FL, USA: CRC Press, 2006.
- [23] R. D. Zimmerman, C. E. Murillo-Sánchez, and R. J. Thomas, "MATPOWER steady-state operations, planning and analysis tools for power systems research and education," *IEEE Trans. Power Syst.*, vol. 26, no. 1, pp. 12–19, Feb. 2011.
- [24] V. Dragalin, A. Tartakovsky, and V. Veeravalli, "Multihypothesis sequential probability ratio tests—Part I: Asymptotic optimality," *IEEE Trans. Inf. Theory*, vol. 45, no. 7, pp. 2448–2461, Nov. 1999.
- [25] S. Fleisher and E. Shwedyk, "A sequential multiple hypotheses test for the unknown parameters of a Gaussian distribution," *IEEE Trans. Inf. Theory*, vol. IT-26, no. 2, pp. 255–259, Mar. 1980.
- [26] V. Dragalin, A. Tartakovsky, and V. Veeravalli, "Multihypothesis sequential probability ratio tests—Part II: Accurate asymptotic expansions for the expected sample size," *IEEE Trans. Inf. Theory*, vol. 46, no. 4, pp. 1366–1383, Jul. 2000.



Yi Huang (S'11) received the B.S. degree in electrical engineering from the University of Arizona, Tucson, AZ, USA, in 2007 and the M.S. degree in electrical engineering from the University of Southern California, Los Angeles, CA, USA, in 2008. He joined the Ph.D. program in 2009 under the supervision of Professor Zhu Han at the University of Houston, Houston, TX, USA.

Prior to entering the University of Houston, he worked as a graduate research assistant under the supervision of University of Southern California Profes-

sor K. Kirk Shung. His current research work includes the application of quickest detection, data mining, machine learning, and signal processing in wireless network, cognitive radio network, and smart grids. He is the author of the paper that won the best paper award in the IEEE Smart Grid Communication 2012.



Mohammad Esmalifalak (S'12) received the M.S. degree in power system engineering from the Shahrood University of Technology, Shahrood, Iran, in 2007. He joined the Ph.D. program in the University of Houston (UH), Houston, TX, USA, in 2010.

From 2010 to 2012, he was a Research Assistant in the Electrical and Computer Engineering department of UH. He is the author of the paper that won the best paper award in the 2012 IEEE Wireless Communications and Networking Conference in Paris, France.

His main research interests include the application of data mining, machine learning, and signal processing in the operation and expansion of the smart grids.



Yu Cheng received the Ph.D. degree in electrical and computer engineering from the University of Waterloo, Ontario, ON, Canada, in 2003.

He is currently an Associate Professor with the Department of Electrical and Computer Engineering, Illinois Institute of Technology, Chicago, IL, USA. His research interests include wireless network performance analysis and network security.

Dr. Cheng was the recipient of the Best Paper Awards from the Conference on Heterogeneous Networking for Quality, Reliability, Security, and

Robustness 2007 and International Conference on Communication 2011, respectively, and of the National Science Foundation CAREER award in 2011. He served as the Symposium Cochair of the IEEE ICC in 2009 and 2012 and the IEEE Global Communications Conference in 2011 and 2013. He is an Associated Editor for the IEEE TRANSACTIONS ON VEHICULAR TECHNOLOGY and IEEE Network.



Husheng Li (S'00–M'05) received the B.S. and M.S. degrees in electronic engineering from Tsinghua University, Beijing, China, in 1998 and 2000, respectively, and the Ph.D. degree in electrical engineering from Princeton University, Princeton, NJ, USA, in 2005.

From 2005 to 2007, he was a Senior Engineer with Qualcomm Inc., San Diego, CA, USA. In 2007, he joined the Electrical Engineering and Computer Science department of the University of Tennessee, Knoxville, TN, USA, as an Assistant Professor. He

is also an international scholar of Kyung Hee University, Seoul, Korea. His research is mainly focused on statistical signal processing, wireless communications, networking, smart grid, and game theory.

Dr. Li was the recipient of the Best Paper Awards of the European Association for Signal Processing Journal of Wireless Communications and Networks 2005, IEEE ICC 2011, and IEEE SmartGridComm 2012, respectively, and of the Best Demo Award of the IEEE Globecom 2010.



Kristy A. Campbell received the Ph.D. degree from the University of California, Davis, CA, USA.

She is currently an Associate Professor with the Department of Electrical and Computer Engineering, Boise State University, Boise, ID, USA. Her research interests are focused on new electronic memory technologies, reconfigurable electronics, and resistance variable devices based on chalcogenide ion-conducting materials. She has over 100 pending/issued patents in the area of chalcogenide materials as used in electronic memory. She has published

more than 20 papers in peer-reviewed journals, three book chapters, and papers for several conference proceedings.



Zhu Han (S'01–M'04–SM'09) received the B.S. degree in electronic engineering from Tsinghua University, Beijing, China, in 1997 and the Ph.D. degree in electrical engineering from the University of Maryland, College Park, MD, USA, in 2003.

From 2006 to 2008, he was an Assistant Professor with Boise State University, Boise, ID, USA. He is currently an Associate Professor with the Department of Electrical and Computer Engineering, University of Houston, Houston, TX, USA. He coauthored papers that won six best paper awards (ICC

2009, International Symposium of Modeling and Optimization in Mobile 2009, Wireless Communications and Networking Conference 2012, International Conference on Wireless Communications Signal Processing 2012, and Smartgridcomm 2012).

Dr. Han was the recipient of the 2010 National Science Foundation CAREER Award as well as the 2011 IEEE Communications Society Fred W. Ellersick Prize.